Heliyon 10 (2024) e39573

Contents lists available at ScienceDirect

Heliyon

journal homepage: www.cell.com/heliyon

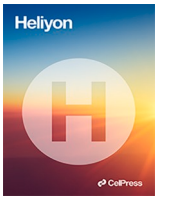

Research article

In-vitro biomineralization of magnesium and copper co-doped wollastonite

M Samuel Collin [a], Balasubramanian Rakshana [a], Jayanthi Abraham [b], Sasikumar S [a,*]

[a] Department of Chemistry, School of Advanced Sciences, Vellore Institute of Technology, Vellore, 632014, Tamil Nadu, India
[b] Microbial Biotechnology Laboratory, School of Bio Sciences & Technology, Vellore Institute of Technology, Vellore, Tamil Nadu, India

ARTICLE INFO

Keywords:
Doping
Biomaterial
Bone tissue engineering
Materials
Wollastonite
Magnesium and copper co-doped
And antibacterial activity

ABSTRACT

Calcium silicate-based ceramics, particularly wollastonite ($CaSiO_3$), are gaining prominence in hard tissue engineering due to their biocompatibility and bioactivity. However, pure wollastonite faces challenges such as insufficient mechanical strength and susceptibility to bacterial colonization. This study addresses these issues by systematically synthesizing magnesium and copper co-doped wollastonite (MgCuW) using the sol-gel combustion technique, aiming to enhance its mechanical stability and antibacterial properties. The average crystalline size of the synthesized materials ranged from 25 to 47 nm. In vitro biomineralization studies showed significant hydroxyapatite deposition, confirming enhanced bioactivity. Antibacterial tests against Gram-positive (S. aureus, S. epidermidis) and Gram-negative (E. coli, P. aeruginosa) bacteria demonstrated superior antibacterial activity with increased copper doping. The results indicate that MgCuW is a promising biomaterial for bone tissue engineering, combining bioactivity and antibacterial efficacy.

1. Introduction

Calcium silicate-based ceramics have gained prominence in hard tissue engineering due to their biocompatibility, bioactivity, and resemblance to natural bone minerals. Wollastonite ($CaSiO_3$), in particular, has shown significant potential for bone regeneration applications owing to its inherent osteogenic properties [1]. However, pure wollastonite has limitations, such as insufficient mechanical strength and susceptibility to bacterial colonization, which restrict its use in load-bearing applications [2]. To address these challenges, researchers have explored co-doping wollastonite with essential elements like magnesium (Mg) and copper (Cu) [3].

The selection of Mg and Cu as co-dopants is based on their complementary roles in enhancing the overall properties of wollastonite. Magnesium is crucial for bone metabolism, as it regulates osteoblast and osteoclast activity, contributing to bone formation and remodeling [4]. Its presence in doped ceramics is known to stimulate osteogenic differentiation and improve the bioactivity of the material, making it highly suitable for bone tissue engineering applications [5]. Moreover, Mg is known to contribute to improved mechanical properties, such as compressive strength, by facilitating better structural integrity of the ceramic matrix [6].

Copper is selected for its potent antibacterial properties, which are critical for preventing microbial infections at implant sites. Copper ions can disrupt bacterial cell membranes and cause DNA damage, reducing the risk of post-surgical infections [7]. This

* Corresponding author.
E-mail address: ssasikumar@vit.ac.in (S. S).

https://doi.org/10.1016/j.heliyon.2024.e39573
Received 3 September 2024; Received in revised form 14 October 2024; Accepted 17 October 2024
Available online 21 October 2024

property is especially important for applications in clinical settings where infection control is a priority. Additionally, Cu is known to promote angiogenesis, which plays a vital role in bone healing by improving blood vessel formation and nutrient supply to the regenerating tissue [8].

The combination of these two dopants, Mg and Cu, allows for a synergistic improvement in both the physicochemical and biological properties of the doped calcium silicate ceramics (DCSCs). Co-doping leads to a balanced release of bioactive ions that enhances osteogenesis, antibacterial activity, and mechanical robustness, making the co-doped ceramics more suitable for clinical applications in bone repair and regeneration. This approach addresses the limitations of pure wollastonite and positions co-doped DCSCs as a

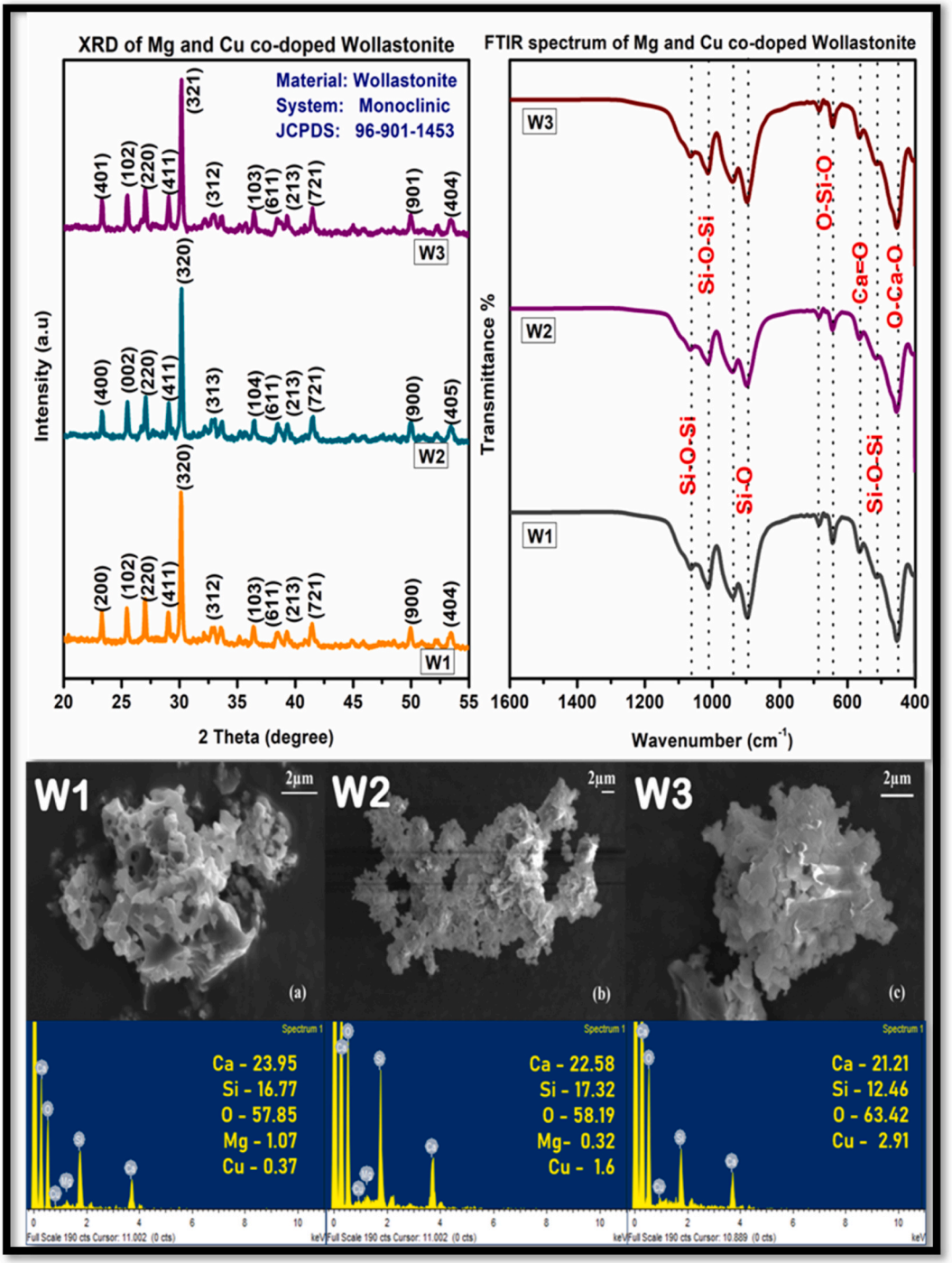

Fig. 1. XRD, FTIR and SEM/EDX of synthesized magnesium and copper co doped wollastonite.

promising alternative to traditional ceramic materials for bone tissue engineering [9].

2. Experimental procedure

Magnesium and copper co-doped wollastonite (MgCuW) was synthesized in three different compositions: W1 ($Ca_{0.94}Mg_{0.05}Cu_{0.01}SiO_3$), W2 ($Ca_{0.93}Mg_{0.05}Cu_{0.02}SiO_3$), and W3 ($Ca_{0.92}Mg_{0.05}Cu_{0.03}SiO_3$). The materials included calcium nitrate tetrahydrate ($Ca(NO_3)_2{\cdot}4H_2O$), magnesium nitrate hexahydrate ($Mg(NO_3)_2{\cdot}6H_2O$), and copper nitrate hexahydrate ($Cu(NO_3)_2{\cdot}6H_2O$). Separate solutions of these nitrates were prepared in beakers, each adjusted to the required molar concentrations based on the targeted compositions. Glycine, used as a fuel, was combined with the nitrate solutions in stoichiometric proportions. The mixtures were stirred at 300 rpm for 30 min to ensure uniform distribution. Tetraethyl orthosilicate (TEOS) was then added dropwise to each solution while maintaining continuous stirring. This step initially created a heterogeneous mixture due to the immiscibility of TEOS and water. To facilitate TEOS hydrolysis and achieve a uniform mixture, 9 mL of concentrated nitric acid was introduced into each solution. The resulting mixture was allowed to rest at room temperature for 24 h, leading to the formation of a gel.

The gels were dried at 120 °C in a hot air oven to remove residual moisture and then aged for 12 h at ambient temperature. These aged gels underwent combustion in a muffle furnace preheated to 400 °C for 30 min, yielding light and porous precursor materials. The resulting precursors were finely ground using an agate mortar and pestle. The powders were subsequently calcined at 800 °C for 6 h to develop the desired crystalline structure. The calcined powders were compressed into pellets using a hydraulic press at 5 tons of pressure for 2 min, following the procedure described by Collin et al. [9]. These pellets were further sintered at 1000 °C for 2 h to improve their densification.The synthesized MgCuW powders and pellets underwent characterization to assess their phase purity, microstructure, and antibacterial properties. The antibacterial activity was tested against two Gram-positive bacterial strains, *Staphylococcus aureus* and *Staphylococcus epidermidis*, as well as two Gram-negative strains, *Escherichia coli* and *Pseudomonas aeruginosa*, using an agar diffusion method as outlined in a previously reported protocol [10].

2.1. Instrumentation techniques

The XRD patterns were recorded by a D8 advance powder X-ray diffractometer (Brucker AXS GmbH, Karlsruhe, Germany) using Cu filter with Kα radiation (wavelength = 1.5406 Å) and an operating voltage of 40 kV and a current of 30 mA. The infrared spectra of the materials were measured by a Shimadzu IRAffinity-1 CE FT-IR Spectrophotometer in the range of 4000–400 cm^{-1} using KBr discs. The XRD patterns were recorded by a D8 advance powder X-ray diffractometer (Brucker AXS GmbH, Karlsruhe, Germany) using Cu filter with Kα radiation (wavelength = 1.5406 Å) and an operating voltage of 40 kV and a current of 30 mA. The infrared spectra of the materials were measured by a Shimadzu IRAffinity-1 CE FT-IR Spectrophotometer in the range of 4000–400 cm^{-1} using KBr discs.

3. Results and discussion

3.1. Characterization

Fig. 1 shows the infrared spectrum of samples W1, W2 and W3. The vibration at 1085 cm^{-1} is attributed to symmetric stretching vibration of Si-O-Si whereas the band at 1061cm^{-1} corresponds to asymmetric stretching vibration of same. Si-O-Si bending vibration occurs at frequencies of 890 cm^{-1} and 930 cm^{-1} [11]. The peaks around 477 cm^{-1} and 455 cm^{-1} represents Ca-O flexural vibration. The peak observed at 510 cm^{-1} corresponds to the characteristic vibrational mode of the O-Si-O linkage, indicating the presence of silicate structures within the samples. Fig. 1 presents the X-ray diffraction (XRD) patterns of magnesium and copper co-doped wollastonite (MgCuW) samples, labeled W1, W2, and W3, which were calcined at 800 °C for 6 h [12]. The diffraction patterns of all compositions closely align with the standard pattern for wollastonite, as provided by JCPDS file number 96-900-5779, confirming that the synthesized material retains the wollastonite phase. A notable observation is the minor shift of the diffraction peaks towards lower 2θ angles with increasing copper content from W1 to W3. This shift can be attributed to changes in the lattice parameters caused by the incorporation of Mg^{2+} and Cu^{2+} ions into the wollastonite structure. The shift towards lower 2θ values is indicative of lattice expansion, which may seem contradictory at first glance, but it is essential to understand the underlying factors contributing to this shift.

In the case of MgCuW, Mg^{2+} and Cu^{2+} ions have been incorporated into the wollastonite lattice. The ionic radii of Mg^{2+} (0.72 Å) and Cu^{2+} (0.73 Å) are slightly larger than that of Ca^{2+} (0.71 Å). The substitution of Ca^{2+} by Mg^{2+} and Cu^{2+} in the crystal structure can create local distortions due to differences in ionic sizes, leading to an increase in the unit cell volume. This expansion results in a longer interplanar spacing, which is manifested as a shift of XRD peaks towards lower 2θ values. Additionally, the co-doping with both Mg and

Table 1
Crystal lattice of synthesized material.

Sample Code	Material doping	Cell Parameters (Å)			Average Crystalline size range (nm)
		a	b	c	
W1	$Ca_{0.94}Mg_{0.05}Cu_{0.01}SiO_3$	15.42232	7.32536	7.06604	25–28
W2	$Ca_{0.93}Mg_{0.05}Cu_{0.02}SiO_3$	15.40541	7.32226	7.06178	27–38
W3	$Ca_{0.92}Mg_{0.05}Cu_{0.03}SiO_3$	15.41214	7.31977	7.06268	35–47

Cu ions can induce strain and create lattice defects, further contributing to this observed shift. Such shifts are often seen in solid-solution systems where substitutional doping alters the lattice dynamics. The average crystallite size (DDD) of the Mg and Cu co-doped wollastonite samples was calculated using Scherrer's formula:

$$D=(k\lambda/\beta \cos \theta)$$

The average crystalline size of all three compositions along with cell parameters is briefed in Table 1. The surface morphology of the calcined Mg and Cu co-doped Wollastonite was studied using SEM-EDX. It was observed that the powder possesses irregular morphology, and the particles were highly agglomerated across all three compositions. The elemental composition was analysed using Energy-Dispersive X-Ray Analysis and the spectrum revealed the presence of all elements.

3.2. Invitro biomineralization

The scaffolds after immersion in SBF for 9 days were analysed using FT-IR and the obtained spectra is shown in Fig. 2. All three compositions W1, W2, W3 expressed remarkable depositions of HAP on analysing the spectrum. The bending vibrational peaks of metal oxides that were observed in pure materials were eliminated thoroughly. The phosphate bonds which confirmed the presence of hap deposition were observed in the range of 557 cm^{-1}, 596 cm^{-1}, 1050 cm^{-1} [14]. Diffraction studies show that the Mg and Cu co-doped Wollastonite had entirely nucleated hydroxyapatite. The apatite peaks precisely matched the hydroxyapatite phase related JCPDS card no. 01-074-0566 [9].

As Cu doping increases, there is an increase in the intensity of apatite peaks from W1 to W2 in Day 6 and Day 9, while it remains consistent going from W2 to W3. Copper is known to enhance bioactivity and this behaviour is in accordance with that [6]. The decrease in the intensity of wollastonite peaks is gradual in W1 and it is prominently present in Day 9 exhibiting slower leaching of ions. In W2 and W3, leaching of ions is faster as the intensity reduces at a pace higher than W1 and the wollastonite peaks gets vanished on Day 9. It is to conclude that leaching of ions varies with difference in doping. The scaffolds were analysed using Scanning electron microscope after immersing them in SBF for 9 days [13]. The micrograph obtained for all three compositions revealed the deposition of HAP. All three compositions exhibit cauliflower like morphology. The EDX spectrum of scaffolds depicts the meticulously covered apatite layer on the surface. The absence of silicon peaks reassures the formation of apatite layer on the surface of the material. Mg and Cu doping influenced the rate of hydroxyapatite (HAp) formation on the material surface, which is a key indicator of bioactivity. Higher Mg content facilitated faster HAp layer formation due to enhanced ionic exchange, while Cu at optimal levels contributed to controlled release of ions that aid in the formation of a stable apatite layer.

3.3. Antibacterial activity

The antibacterial effectiveness of Mg-Cu-W was evaluated against clinical pathogens: S. aureus, P. aeruginosa, S. epidermidis, and E. coli, with results shown in Table 2. The antiba [12] cterial activity increased with the concentration of Cu (Fig. 3), showing no

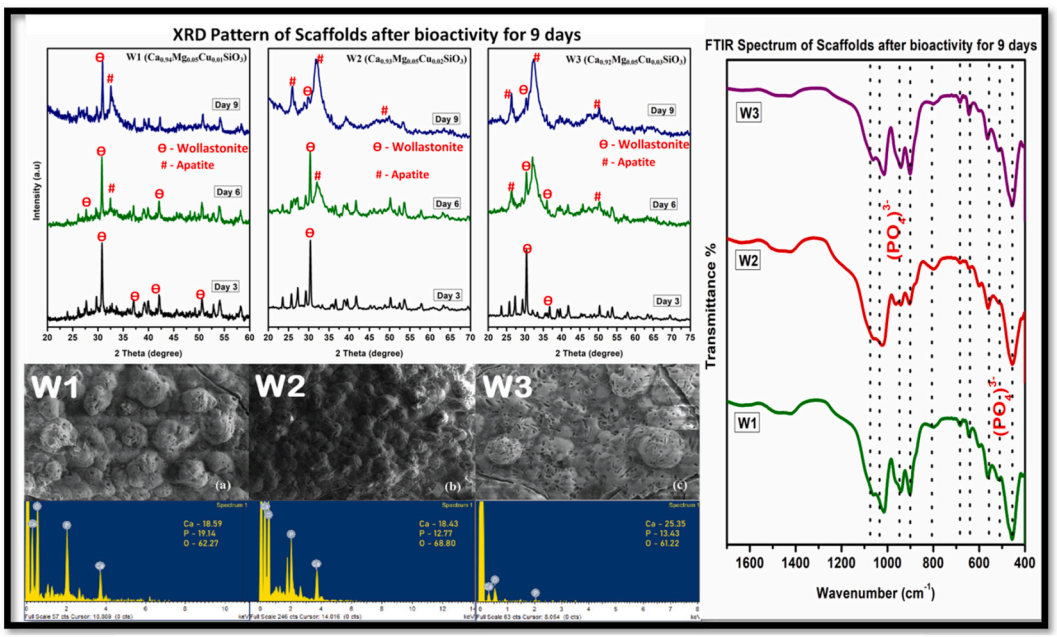

Fig. 2. XRD, FTIR and SEM/EDX of wollastonite scaffolds immersed in SBF for over 9 days.

exceptional resistance among the isolates. W3 exhibited excellent activity against E. coli. SEM micrographs (Fig. 3) depict the clustering of MgCuW around S. aureus and E. coli cells, causing cell surface distortion. Magnesium ions, acting as cofactors in enzymatic reactions, decrease bacterial adherence and impair biofilm formation at higher concentrations. Previous studies by Murthi et al. [15] reported Cu-doped wollastonite's efficacy against E. coli and S. aureus, corroborating the findings of Swamiappan et al. [16], who reported significant antibacterial activity of wollastonite against both Gram-positive and Gram-negative bacteria. The ability of bioceramic to trigger the release of calcium ions leads to membrane depolarization and changes in cell permeability, resulting in cell death due to its antimicrobial properties. An excess of calcium ions can lead to either necrosis or initiate apoptotic cell death, adding to its strong bactericidal effects [17].

Kharouf et al. (2020) compared the antibacterial activity of two calcium silicate-based sealers—Ceraseal (CS) and BioRoot (BR)—showed that both demonstrated no effectiveness against *Enterococcus faecalis* after a 3-h period [18]. Nevertheless, BR exhibited a notably stronger antibacterial impact (60 % bactericidal activity) than CS after 24 h. Another study Shi et al. (2016) by validates that hydroxyapatite bioceramic substituted with silver enhanced the antibacterial property, which also suggested that doping can lead to enhanced antibacterial property [19]. Samples with higher Cu content exhibited increased antibacterial activity, as Cu ions can disrupt bacterial membranes and inhibit growth. However, balancing Cu concentration was crucial to maintaining the material's biocompatibility while achieving effective antibacterial properties. The current study's results findings evinced higher antibacterial activity when compared to other researches, confirming the potential of MgCuW as an effective antibacterial biomaterial.

3.4. Mechanical studies

The mechanical stability of magnesium and copper co-doped wollastonite samples soaked in Simulated Body Fluid (SBF) for 9 days was evaluated by measuring compressive strength and Young's modulus, as shown in Fig. 4. Among the three compositions, W1 exhibited the highest compressive strength at 79 MPa, while W2 and W3 demonstrated a decrease in strength by 22 % and 24 %, respectively. A similar trend was observed in the Young's modulus values. The compressive strength of W1 is approximately 5 times higher than the maximum strength of cancellous bone and 1.5 times lower than the minimum strength of cortical bone, highlighting its potential for load-bearing applications [20].

The mechanical properties of in-vitro scaffolds are influenced by the balance between degradation, which decreases the material's strength, and apatite formation, which enhances strength. The dominant process dictates the overall mechanical strength of the scaffolds. XRD analysis of the in-vitro scaffolds revealed that W1 exhibited a gradual decrease in wollastonite peaks and a consistent increase in apatite peaks, indicating a balanced degradation and apatite formation [21]. In contrast, W2 and W3 displayed a rapid decline in the intensity of wollastonite peaks, especially from day 6 to day 9, suggesting a higher degradation rate. This rapid degradation resulted in lower compressive strength for W2 and W3g significantly improved the mechanical strength of the bioceramics, making them more suitable for load-bearing applications. Adjusting the Mg content allowed for the optimization of toughness and resistance to mechanical stress. However, higher levels of Cu doping led to a slight reduction in strength, which required careful balancing to maintain adequate mechanical integrity [22].

Biodegradability studies supported these findings, as W1 demonstrated a balanced rate of degradation and apatite formation, leading to stable mechanical properties. In contrast, W2 and W3 experienced accelerated degradation between days 6 and 9, increasing porosity and weakening the scaffold structure, which was not adequately compensated by apatite formation, resulting in reduced mechanical strength.

4. Conclusion

Magnesium and copper co-doped wollastonite (MgCuW) synthesized using the sol-gel combustion technique, demonstrating its potential as an advanced biomaterial for hard tissue engineering. The characterization of MgCuW through XRD, FT-IR, and SEM-EDX confirmed the formation of wollastonite with dopant-induced structural modifications, resulting in crystalline sizes between 25 and 47 nm. In vitro biomineralization assays revealed extensive hydroxyapatite formation on the scaffold surfaces, indicating excellent bioactivity. Antibacterial testing showed that MgCuW exhibited significant activity against both Gram-positive and Gram-negative bacteria, with increased copper content enhancing this effect. Notably, W3 with higher copper concentration displayed the highest

Table 2
Inhibition of bacterial growth by magnesium copper co-doped wollastonite.

Sample code	% inhibition of bacterial growth			
	S. aureus	P. aeruginosa	S. epidermidis	E. coli
W1 (0.5 mg/L)	19.78	12.91	9.86	8.73
W1 (1 mg/L)	22.76	16.29	20.71	11.79
W1 (2 mg/L)	23.29	23.68	29.27	11.79
W2 (0.5 mg/L)	20.67	18.91	22.33	25.37
W2 (1 mg/L)	23.7	23.86	23.79	28.91
W2 (2 mg/L)	31.68	26.13	23.79	32.91
W3 (0.5 mg/L)	29.78	25.67	9.32	28.76
W3 (1 mg/L)	34.78	26.81	17.81	47.90
W3 (2 mg/L)	37.36	32.72	23.78	59.09

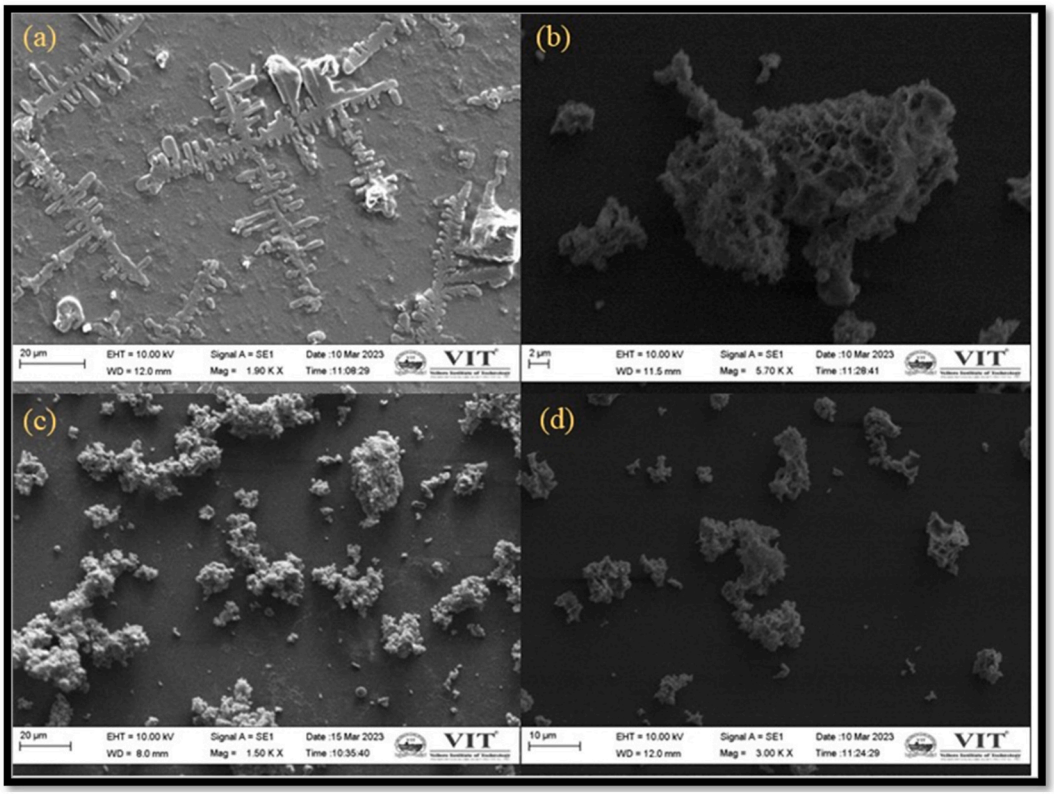

Fig. 3. SEM micrograph of antibacterial assay of Mg-Cu-Ws (W3) against clinical pathogens: (a) *Escherichia coli* (control), (b) *E. coli* post treatment, (c) *Staphylococcus aureus* (control), (d) *S. aureus* post treatment.

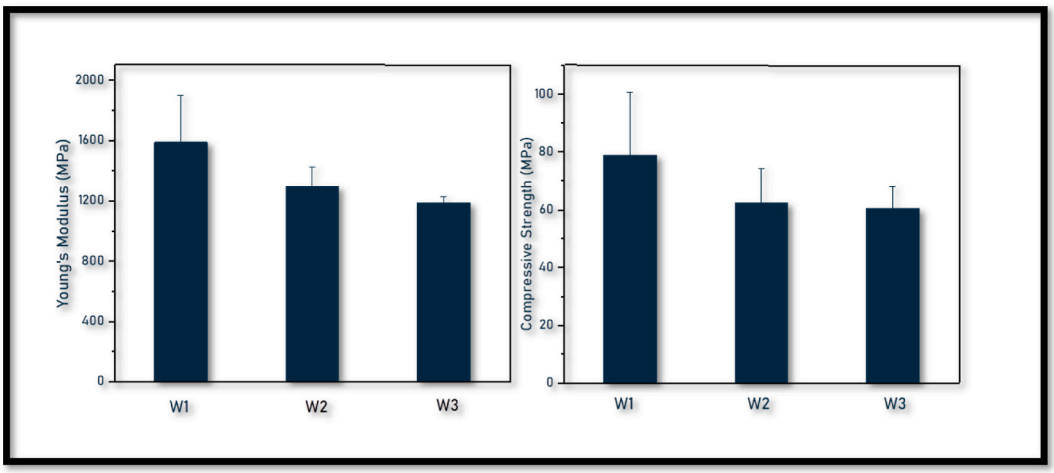

Fig. 4. Compression strength and Young; s modulus of MgCuW.

antibacterial efficiency, particularly against E. coli. These findings highlight the dual benefits of Mg and Cu doping in enhancing both the mechanical and biological properties of wollastonite, making MgCuW a strong candidate for clinical applications in bone repair and regeneration. Further studies focusing on in vivo performance and long-term stability of MgCuW scaffolds could pave the way for their integration into clinical practice.

CRediT authorship contribution statement

M Samuel Collin: Writing – original draft, Methodology. **Balasubramanian Rakshana:** Investigation. **Jayanthi Abraham:** Supervision. **Sasikumar S:** Writing – review & editing, Conceptualization.

Data statement

The data that has been used is confidential. Data made available on request to the corresponding author.

Declaration of competing interest

The authors declare the following financial interests/personal relationships which may be considered as potential competing interests:Sasikumar S reports financial support was provided by Vellore Institute of Technology. If there are other authors, they declare that they have no known competing financial interests or personal relationships that could have appeared to influence the work reported in this paper.

References

[1] George Gonçalves dos Santos, et al., Wollastonite and tricalcium phosphate composites for bone regeneration, Research, Society and Development 11 (9) (2022), 12011931662-e12011931662.
[2] M. Samuel Collin, Sasikumar Swamiappan, Effect of fuel on biomineralization of merwinite, Mater. Lett. 304 (2021) 130660.
[3] Teshome Abdo Segne, Siva Rao Tirukkovalluri, Subrahmanyam Challapalli, Studies on characterization and photocatalytic activities of visible light sensitive TiO2 nano catalysts co-doped with magnesium and copper, Int. Res. J. Pure Appl. Chem. 1 (3) (2011) 84–103.
[4] F. Khorashadizade, et al., Overview of magnesium-ceramic composites: mechanical, corrosion and biological properties, J. Mater. Res. Technol. 15 (2021) 6034–6066.
[5] Kaushik Sarkar, et al., Effects of Sr doping on biodegradation and bone regeneration of magnesium phosphate bioceramics, Materialia 5 (2019) 100211.
[6] Gokhan Acikbas, Nurcan Calis Acikbas, Copper oxide-and copper-modified antibacterial ceramic surfaces, J. Am. Ceram. Soc. 105 (2) (2022) 873–887.
[7] Saeid Kargozar, et al., Copper-containing bioactive glasses and glass-ceramics: from tissue regeneration to cancer therapeutic strategies, Mater. Sci. Eng. C 121 (2021) 111741.
[8] Panmella Pereira Maciel, et al., Use of strontium doping glass-ceramic material for bone regeneration in critical defect: in vitro and in vivo analyses, Ceram. Int. 46 (16) (2020) 24940–24954.
[9] M. Samuel Collin, et al., Solution combustion synthesis of functional diopside, akermanite, and merwinite bioceramics: excellent biomineralization, mechanical strength, and antibacterial ability, Mater. Today Commun. 27 (2021) 102365.
[10] Samuel M. Collin, et al., Thermo-mechanical stability and antibacterial activity of merwinite derived from different fuels, J. Mater. Res. 38 (23) (2023) 5045–5054.
[11] Sherlin Joseph, Sasikumar Swamiappan, Preparation and characterization of diopside-wollastonite composite for orthopedic application, Silicon 16 (3) (2024) 1161–1171.
[12] Y.E. Greish, P.W. Brown, Characterization of wollastonite-reinforced HAp–Ca polycarboxylate composites, J. Biomed. Mater. Res.: An Official Journal of The Society for Biomaterials, The Japanese Society for Biomaterials, and The Australian Society for Biomaterials and the Korean Society for Biomaterials 55 (4) (2001) 618–628.
[13] Joon Fatt Wong, et al., Thermal and flammability properties of wollastonite-filled thermoplastic composites: a review, J. Mater. Sci. 56 (2021) 8911–8950.
[14] Sherlin Joseph, et al., Investigation on the compatibility of forsterite for tissue engineering application, Mater. Lett. 308 (2022) 131188.
[15] S. Azeena, et al., Antibacterial activity of agricultural waste derived wollastonite doped with copper for bone tissue engineering, Mater. Sci. Eng. C 71 (2017) 1156–1165.
[16] Rajan Choudhary, et al., Antibacterial forsterite (Mg2SiO4) scaffold: a promising bioceramic for load bearing applications, Bioact. Mater. 3 (3) (2018) 218–224.
[17] B. Cabal, L. Alou, F. Cafini, R. Couceiro, D. Sevillano, L. Esteban-Tejeda, J.S. Moya, A new biocompatible and antibacterial phosphate free glass-ceramic for medical applications, Sci. Rep. 4 (1) (2014) 1–9.
[18] N. Kharouf, Y. Arntz, A. Eid, J. Zghal, S. Sauro, Y. Haikel, D. Mancino, Physicochemical and antibacterial properties of novel, premixed calcium silicate-based sealer compared to powder–liquid bioceramic sealer, J. Clin. Med. 9 (10) (2020) 3096.
[19] C. Shi, J. Gao, M. Wang, Y. Shao, L. Wang, D. Wang, Y. Zhu, Functional hydroxyapatite bioceramics with excellent osteoconductivity and stern-interface induced antibacterial ability, Biomater. Sci. 4 (4) (2016) 699–710.
[20] Z. Hong, P. Zhang, C. He, Development and application of 3D printed scaffolds with osteoinductivity for bone tissue engineering, J. Mater. Chem. B 4 (2) (2016) 2393–2403.
[21] R. Detsch, A.R. Boccaccini, The role of osteoclasts in bone tissue engineering, Journal of Tissue Engineering and Regenerative Medicine 5 (10) (2011) e163–e173.
[22] A.G. Gristina, J.W. Costerton, Bacterial adherence to biomaterials and tissue, Biomaterials 6 (6) (1985) 403–408.